

The influence of carbide coarsening on the friction properties of thermally affected 9–12 wt. % Cr steels

**I. Velkavrh^{1*}, F. Kafexhiu², S. Klien¹, F. Ausserer¹, J. Voyer¹, A. Diem¹,
B. Podgornik²**

¹ V-Research GmbH, Stadtstrasse 33, 6850 Dornbirn, Austria

² Institute of Metals and Technology, Lepi pot 11, 1000 Ljubljana, Slovenia

*Corresponding author: igor.velkavrh@v-research.at

Abstract. The purpose of the present study is to evaluate the influence of tempering-induced carbide coarsening in the heat affected zone of two grades of 9–12 wt. % Cr steels, X20 and P91, on their friction properties. In order to compare the frictional properties of the selected microstructures without and with the presence of oxides on the contacting surfaces, friction tests were performed under Ar atmosphere and in air. It was observed that after tempering, coefficient of friction increases for both steels in both atmospheres. This deterioration of friction properties after tempering is probably due to the precipitation of carbides, which acted as mechanical anchors and/or increased the surface energy of steel. Since neither the number of carbides nor their size distribution showed an influence on the friction properties of the selected steels, it is presumed that the minor differences between the friction properties of the tempered X20 and P91 steels are primarily related to their oxidative properties.

1. Introduction

9–12 wt. % Cr martensitic alloy steels are used in vital parts of fossil-fuel power plants, such as turbines, headers, main steam pipes, etc., due to their good mechanical properties and corrosion resistance at elevated temperatures. Although sliding typically does not occur in these applications, components made of these steels may come into sliding contact with neighboring elements under special conditions such as overload or start-ups/shut-downs of fossil-fuel power plants. For instance, steam turbine valve seat materials require an excellent resistance to galling, wear, oxidation and thermal expansion. Namely, it was already reported that most of the turbine overspeed incidents have been caused by valves failing to close or due to the failure of the overspeed protection mechanism [1].

Welding is a major joining and repair technology for 9–12 wt. % Cr steels used for high temperature power plant structures. For applications with elevated temperatures in which martensitic 9–12 wt. % Cr steels are typically used, different temperature-induced processes occur, including coarsening of carbide particles, which significantly affect the material's mechanical properties [2–4]. In general, precipitation of carbides during tempering increases toughness and tensile strength of steels [5–7].

For Inconel 600 mill-annealed alloy, it was already reported that carbide precipitation after aging treatment strongly affected its fretting wear behavior as wear volume increased with the increase of carbides and that carbide precipitation slightly increased the coefficient of friction [8].



In a previous study of the present authors [9], it was observed that X20 steel provided better wear resistance than P91 steel, which was attributed to the less pronounced tempering-induced coarsening and the correlated smaller dissolution of carbide particles. Namely, after tempering, the number of carbide particles was typically higher in the steel X20 than in the P91 and at the same time, a higher number of medium-sized carbide particles (100–200 nm) was observed in the steel X20, while in the steel P91, a higher number of small-sized carbide particles was found (0–50 nm). It was presumed that the less pronounced coarsening, i.e. higher stability of carbide particles in X20 steel is related to its higher carbon content (Table 1).

Alongside the wear resistance, coefficient of friction is another important property to be considered for sliding conditions. However, in the available literature, no studies on the influence of carbide coarsening on the friction properties of 9–12 wt. % Cr steels can be found. The purpose of the present study is to further evaluate the potential of the X20 and P91 steels as materials for applications operating under a combined effect of mechanical wear and alternating high/low temperature conditions. The influence of tempering-induced carbide coarsening on the friction properties of the weld heat affected regions of the selected materials and microstructures is analyzed.

2. Experimental

2.1. Materials preparation

Two grades of creep-resistant 9–12 wt. % Cr steels, X20 and P91, were used in this study. In Table 1, chemical composition of both steels according to the DIN EN 10216-2 standard is given. For the heat treatment procedures, cylindrical samples with a diameter of 13 mm were used. In order to obtain the microstructure of tempered martensite, a routine heat treatment was performed. It started with austenitizing at 1050°C for 30 minutes in order to dissolve the carbide particles in austenite. Afterwards, steels were rapidly cooled (quenched) in oil, which led to a relatively brittle and hard martensitic microstructure. Finally, tempering at 810°C for 30 minutes was performed followed by air-cooling, resulting in a tempered martensitic microstructure, which represented the basis (parent metal, α) for further heat treatment processes.

Additional heat-treatment procedures with the aim to simulate two different HAZ regions, i.e., inter-critical ($\alpha+\gamma$) and coarse-grained (γ) microstructures, were carried out. The $\alpha+\gamma$ microstructure was obtained by keeping the samples in the temperature range of $Ac_1 < T < Ac_3$, i.e. at 845°C, for 60 minutes. The γ microstructure was obtained by keeping the samples above the Ac_3 temperature, i.e. at 1000°C, for 30 minutes. After keeping the samples at the selected temperatures over the selected time periods, the samples were rapidly cooled in air.

The final part of the heat treatment process was performed in order to induce the changes of size, distribution and mutual spacing of carbide particles. It consisted of tempering of the $\alpha+\gamma$ and γ microstructures of both steels for 1 week and 1 month (168 h and 720 h) at 650°C and 750°C.

After the heat treatment, samples were longitudinally cut in order to obtain flat surfaces for microstructure characterization and wear tests. Samples were first ground with silicon carbide paper to a sufficient depth in order to remove any unrepresentative surface and then polished in several steps in order to achieve a surface roughness of $R_a < 0.01 \mu\text{m}$.

Table 1. Chemical composition of X20 and P91 steels according to the DIN EN 10216-2 standard.

El. (wt. %)	C	Si	Mn	P	S	Cr	Ni	Mo	V	Cu	Nb	Al	N
X20	0.17	max 0.5	max 1.0	max 0.03	max 0.03	10.0	0.30	0.8	0.25	-	-	-	-
	- 0.23					- 12.5	- 0.80	- 1.2	- 0.35				
P91	0.08	0.20 -	0.30 -	max 0.02	max 0.01	8.00	max	0.85	0.18	max	0.06	max	0.03
	- 0.12					- 9.50	0.4	- 1.05	- 0.25	0.30	- 0.10	0.04	- 0.07

2.2. Microstructure characterisation

Microstructure changes due to different heat treatment procedures were evaluated via the analysis of micrographs obtained with JEOL JSM-6500F (JEOL Ltd., Japan) scanning electron microscope (SEM). In order to obtain the number, average spacing and size values of carbide particles, image analyses of SEM micrographs were carried out using FIJI (ImageJ) software [10]. Number density, average spacing and size distribution of carbide particles were evaluated and are presented in Table 2 for the steel X20 and in Table 3 for the steel P91. A detailed analysis of microstructural changes is presented in [9].

Table 2. Number density, average spacing and percentage size distribution of carbide particles in the steel X20 after tempering for different times at different temperatures.

X20	Tempering	No. particles per 100 μm^2	Average spacing (μm)	Percentage size distribution (%)						
				0–50 nm	50–100 nm	100–200 nm	200–300 nm	300–400 nm	400–500 nm	500–600 nm
$\alpha+\gamma$	168 h / 650°C	1262	0.17 ± 0.06	26	25	40	9	1	0	0
	720 h / 650°C	917	0.19 ± 0.07	23	18	41	15	3	0	0
	168 h / 750°C	646	0.22 ± 0.09	20	23	36	18	3	1	0
	720 h / 750°C	505	0.24 ± 0.13	26	22	26	19	5	2	1
γ	168 h / 650°C	1033	0.18 ± 0.07	16	29	45	9	1	0	0
	720 h / 650°C	852	0.20 ± 0.08	8	24	53	12	2	0	0
	168 h / 750°C	588	0.22 ± 0.10	7	27	48	14	3	1	0.15
	720 h / 750°C	529	0.23 ± 0.12	29	17	29	16	7	2	0

Table 3. Number density, average spacing and percentage size distribution of carbide particles in the steel P91 after tempering for different times at different temperatures.

P91	Tempering	No. particles per 100 μm^2	Average spacing (μm)	Percentage size distribution (%)						
				0–50 nm	50–100 nm	100–200 nm	200–300 nm	300–400 nm	400–500 nm	500–600 nm
$\alpha+\gamma$	168 h / 650°C	1099	0.15 ± 0.08	50	21	23	6	0	0	0
	720 h / 650°C	948	0.16 ± 0.09	44	27	24	5	0	0	0
	168 h / 750°C	594	0.21 ± 0.12	35	26	25	11	2	1	0
	720 h / 750°C	207	0.36 ± 0.25	35	25	20	12	4	2	1
γ	168 h / 650°C	1061	0.18 ± 0.08	37	23	28	10	1	0	0
	720 h / 650°C	600	0.21 ± 0.11	31	19	31	15	3	1	0
	168 h / 750°C	491	0.24 ± 0.11	20	38	25	12	3	2	0
	720 h / 750°C	377	0.26 ± 0.13	48	26	16	6	3	1	0

2.3. Friction tests

Friction tests were performed on an oscillating tribological test rig (SRV4, Optimol Instruments Prüftechnik GmbH, Germany) with a ball-on-flat testing geometry using DIN 100Cr6 steel (AISI 52100 equivalent) balls with a diameter of 10 mm, sliding against the flat side of a half-cylinder. The balls had a hardness of 62.5 ± 2 HRC (corresponds to approximately 760 HV) and a roughness of R_a 0.02 μm . The initial hardness of the steels X20 and P91 was significantly lower than the hardness of the ball and had values of 238 HV and 228 HV, respectively.

In order to compare the frictional properties of the selected microstructures without and with the presence of oxides on the contacting surfaces, friction tests were performed under Ar atmosphere and in air. In air, metallic surfaces are covered with a thin layer of oxides which usually possess more favorable tribological properties than non-oxidized metallic surfaces [11]. The properties of nascent,

non-oxidized metallic surfaces can be studied only in non-reactive atmospheres such as Ar, where the oxide layers cannot reform after removal (due to the high reactivity of nascent metallic surfaces, oxide layers normally form very rapidly – in e.g., 10^{-2} s at a pressure of 10^{-4} Torr [12]).

Before starting the friction tests, a flow of Ar gas with a gas pressure of 0.05 bar at the gas-bottle outflow was directed onto the contact for 3 minutes in order to remove any adsorbed atmospheric contaminations. After 3 minutes of flushing with Ar gas, the friction test was started and after 2 minutes of sliding, Ar gas flow was stopped so that air could come into the contact. Afterwards, the test was conducted for an additional duration of 2 minutes.

The frequency of the oscillating motion was 0.25 Hz with amplitude of 2 mm resulting in a maximum sliding velocity of 1.6 mm/s (ball movement is sinusoidal). A normal load of 30 N was applied, corresponding to 0.98 GPa and 1.46 GPa of mean and maximal Hertzian contact pressures respectively. It should be noted that the calculated Hertzian contact is significantly higher than the yield strength of both materials and doesn't correspond to the actual contact pressure. Namely, the Hertzian contact pressure considers only the elastic deformation of the material; hence when the yield strength of the material is exceeded, the actual contact pressure does not continue to increase exponentially, but remains more or less constant due to the plastic flow of the material and the related increase of the contact surface.

The coefficient of friction was calculated as the ratio of the tangential force (friction force) and the normal force. The maximum coefficient of friction occurred at the beginning of each stroke, where a break-away friction was typically observed (Figure 1). This maximum value corresponds to the so-called static coefficient of friction and was regarded as the coefficient of friction of interest. The measurement presented in Figure 1 was performed under Ar atmosphere. It should be noted that due to the high adhesion between the ball and the flat surface, after the end of the oscillating cycle, at 6 s, the ball did not yet return into its initial position although the ball holder did. Hence, due to the residual stresses between the ball holder and the ball, coefficient of friction was not zero, but gradually decreased to zero as the ball was slowly dragged into its initial position, which typically required 2–3 s after the end of an oscillating cycle. Therefore, after each oscillating cycle a waiting time of 12 s was applied.

Each microstructure was tested 3 times in order to ensure the repeatability of the measured friction curves.

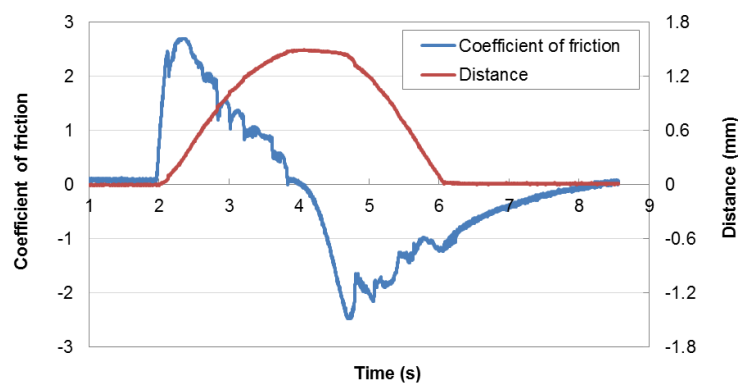


Figure 1: Typical friction signal for a single oscillating cycle.

3. Results

Figure 2 shows typical friction curves obtained in Ar and air atmospheres. Each friction point represents an average value from 3 tests. From Figure 2 it is clear that for both steels and microstructures, relatively low friction values in the range from 0.3 to 1 were initially measured. Afterwards, within the first 5 cycles, i.e. within the first 1 min of test, they increased to values higher than 2. This shows that the surfaces were initially covered with a frictionally favorable oxide layer, which was quickly removed due to sliding under high contact pressure. After the removal of the oxide

layer, nascent steel surfaces, which could not re-oxidize under Ar atmosphere, came into contact, resulting in high adhesion and consequently high friction (coefficients of friction between 2.2 and 2.7). After 2 min of test, when surfaces were exposed to air, coefficients of friction started to decrease due to the re-oxidation of the surfaces and reached values between 1.5 and 2.5 at the end of the test. Friction values were generally around 20% lower in air than in Ar atmosphere.

From Figure 2 it can be also observed that for both steels and microstructures, friction values in both atmospheres were generally the lowest for the samples before tempering, i.e. in the initial state. This indicates that tempering deteriorated the friction properties of the selected materials, possibly due to a higher amount of carbide precipitates which either acted as mechanical anchors and/or increased the surface energy of the samples.

For the steel X20, both microstructures, $\alpha+\gamma$ and γ , showed similar friction curves before tempering (Figures 2a and b). On the other hand, for the steel P91, coefficient of friction was lower for γ than for $\alpha+\gamma$ microstructure, which was especially pronounced in air where the difference was around 15%. This observation suggests that in the initial state, the γ microstructure of the steel P91 had a lower adhesion and/or surface energy than the $\alpha+\gamma$ microstructure. In air, where a more pronounced difference was observed, this was probably correlated with properties of the surface oxides. On the other hand, in Ar atmosphere where the difference was minor, this could be correlated with the distribution of carbides or with the crystalline properties of the material.

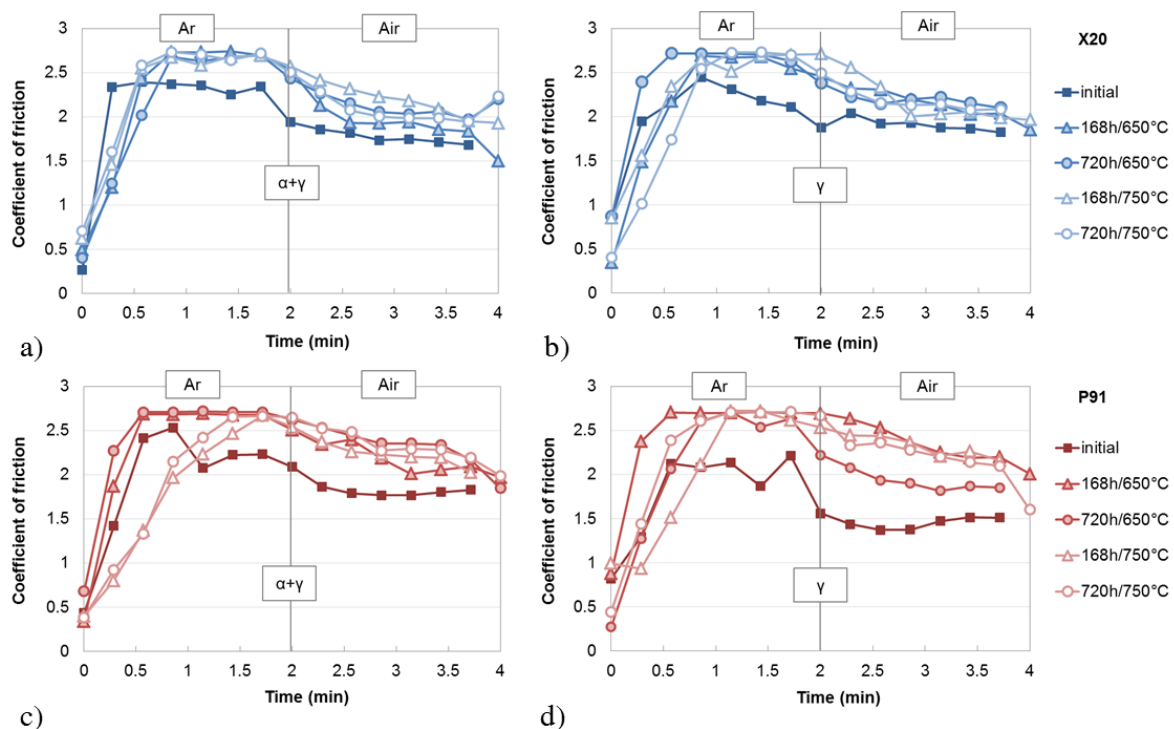


Figure 2: Typical friction curves from Ar and air atmospheres: (a) $\alpha+\gamma$ microstructure of the steel X20, (b) γ microstructure of the steel X20, (c) $\alpha+\gamma$ microstructure of the steel P91 and (d) γ microstructure of the steel P91.

After tempering, coefficient of friction increased for both steels in both atmospheres. The increase of friction due to tempering was more pronounced for the steel P91 (Figures 2c and 2d) than for the steel X20 (Figures 2a and 2b), which shows that the surface properties of the steel X20 were less affected by tempering than those of the steel P91. Furthermore, the changes in friction values due to different tempering conditions (time and temperature) were more pronounced for the P91 than for the steel X20, which was especially true for the γ microstructure.

It is interesting to note that after tempering, the initial increase of friction in Ar atmosphere was typically faster for the microstructures tempered at 650°C as compared to those tempered at 750°C, which was especially pronounced for the steel P91. Namely, for both microstructures of the steel P91 tempered at 650°C, the maximum friction was reached already after 0.5 to 0.8 min, while with the microstructures tempered at 750°C the maximum friction was reached first after around 1 to 1.5 min. This behavior could be the result of different carbide/nitride and microstructure morphology due to different precipitate coarsening kinetics at two different temperatures. For the steel X20, a similar trend was observed; however it was less pronounced when compared to the steel P91. This indicates that the surface morphology of the steel X20 was less affected by high temperature tempering as that of P91. Possibly, this may have affected also the surface oxidation of P91 samples, which would have been more pronounced due to its lower Cr content (Table 1) – generally friction is lower when more iron oxides form on the steel surfaces. The maximum values of friction in Ar atmosphere were similar for both steels and microstructures.

In air, coefficient of friction showed only minor differences depending on the tempering conditions. A notable influence of tempering time was observed only for the $\alpha+\gamma$ microstructure of the steel X20 tempered at 750°C and for the γ microstructure of the steel P91 tempered at 650°C – in both cases, friction decreased with tempering time. For all other microstructures, the influence of tempering time on friction was negligible. Similarly, the influence of tempering temperature was observed only for the $\alpha+\gamma$ microstructure of the steel X20 tempered for 168 h and for the γ microstructure of the steel P91 tempered for 720 h – in both cases, friction increased with tempering temperature. For all other microstructures, the influence of tempering temperature on friction was negligible.

Figure 3 shows coefficient of friction values measured in air in dependence of the number of carbide particles for both steels and microstructures after tempering. The number of carbides can be found in Tables 2 and 3, while the presented coefficient of friction values correspond to the values measured at 3.1 min of testing time (Figure 2). It is believed that at this time interval (3.1 min), surfaces were fully re-oxidised and the contact conditions have stabilized themselves. It is interesting to note that a linear regression of all coefficient of friction values shows an increasing trend with decreased number of carbide particles (growth of larger particles on the account of dissolution of smaller particles – both effects were promoted with tempering temperature and tempering time). Although the observed decrease was not very pronounced (within the standard deviation values), this indicates that a reduced number of carbides, which is related to carbide coarsening, increased the friction of the tempered samples. However, it should be noted that for the presented linear regression, two measurements which were significantly outside of the observed trend were omitted: $\alpha+\gamma$ microstructure of the steel P91 tempered for 720h at 650°C and γ microstructure of the steel P91 tempered for 720h at 650°C.

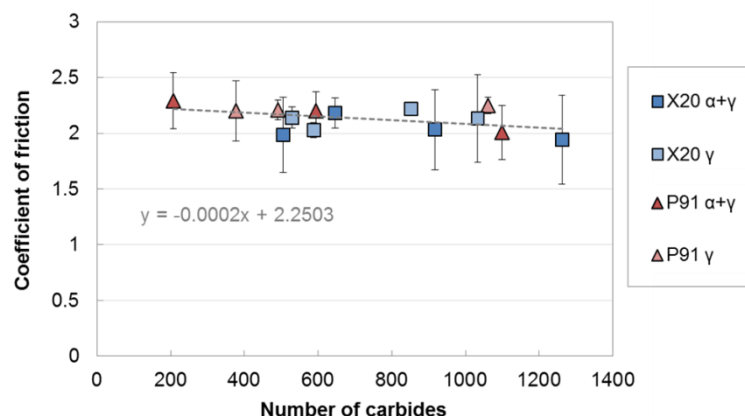


Figure 3: Linear regression of coefficient of friction values measured in air at 3.1 min of testing time for both steels and microstructures after tempering in dependence of the number of carbide particles.

4. Discussion

In the previous study of the authors [9], it was observed that the wear behavior of weld heat affected zones of the steels X20 and P91 is influenced by tempering and that the wear was typically lower for the tempered microstructures than for the microstructures in initial state, i.e. before tempering (exception was γ microstructure of the steel X20). Furthermore, lower wear occurred when a higher number of medium- and large-sized carbide particles were present in the microstructure. In the present study, it was shown that the influence of tempering on the frictional properties of these microstructures is contradictory to the influence on wear, since after tempering, the friction increased for all microstructures. This is attributed to the carbide precipitation where the carbides could either act as mechanical anchors and/or increase the surface energy of the samples. This conclusion is also supported by observations from other authors which reported that the carbide precipitation increased the friction of Inconel 600 mill-annealed alloy [8].

Although for the steel P91, coarsening and dissolution of carbide particles due to tempering was more pronounced than for the steel X20, which is probably correlated with the higher C content in the latter, it is interesting to note that for the steel P91, the increase of friction due to tempering was slightly more pronounced than for the steel X20.

Tempering at a higher temperature probably provided different carbide/nitride and microstructure morphology, resulting from higher coarsening kinetics and lower thermal stability of precipitates. Namely, for both steels, samples tempered at a higher temperature required a longer time for reaching the maximum friction in Ar atmosphere. This could be attributed to higher solid solubility of carbide/nitride forming elements at higher temperatures, and therefore higher solid solution hardening. This effect was stronger for the steel P91 as compared to the steel X20; the difference could also be correlated with a lower oxidation stability of the steel P91 due to its lower Cr content (Table 1).

While in Ar atmosphere the maximum friction values were similar for all microstructures, in air, minor differences were observed but only for some microstructures ($\alpha+\gamma$ microstructure of the steel X20 and γ microstructure of the steel P91). In air, coefficient of friction of both steels and microstructures showed a decreasing trend with an increased number of carbide particles, which indicates that the reduced number of carbides due to carbide coarsening on the account of dissolution of smaller particles, increased the friction properties of the tempered steels.

In Figure 4, the influence of the number of carbides (related to carbide coarsening) on friction and wear of the steels X20 and P91 is schematically presented. The wear curve was estimated on the basis of the results from the previous study [9]. Generally, wear was low when the number of carbide particles due to coarsening was small. However, if the number of carbide particles decreased too much due to their complete dissolution, this significantly increased wear. On the other hand, coefficient of friction showed a tendency to linearly decrease with the increased number of carbides, but this was true only for air, which indicates that changes of the surface morphology due to carbide precipitation have also affected the properties of the surface oxides of the tempered steel samples.

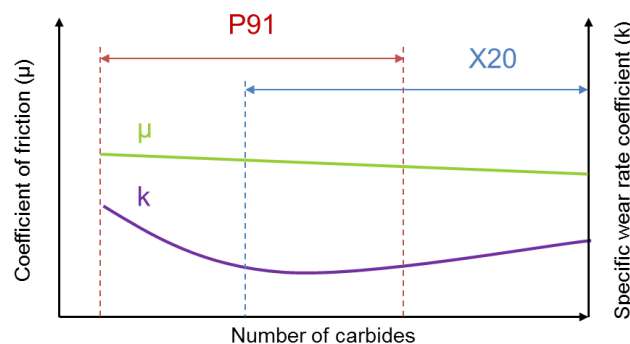


Figure 4: Schematic representation of the influence of the number of carbides (related to carbide coarsening) on friction and wear of the steels X20 and P91.

5. Conclusions

1. After tempering, coefficient of friction increased for both steels in both atmospheres (Ar and air). It is presumed that the deterioration of friction properties after tempering occurs primarily due to carbide precipitation, where carbides act either as mechanical anchors and/or increase the surface energy of the materials.
2. For both steels, samples tempered at a higher temperature required longer time for reaching the maximum friction in Ar atmosphere, which could be attributed to higher solid solubility of carbide/nitride forming elements at higher temperatures, and therefore higher solid solution hardening. This effect was stronger for P91 steel, and was possibly correlated also with the lower oxidation stability of this steel due to its lower Cr content.
3. In Ar atmosphere, the maximum friction values were similar for both steels and microstructures, while in air, more pronounced differences were observed for different microstructures and tempering conditions. Since friction is generally lower when more iron oxides form on the steel surfaces, it is possible that the changes of the surface morphology due to carbide precipitation have affected the properties of the surface oxides of the tempered steel samples.
4. Coefficient of friction showed a light tendency to linearly decrease with the increased number of carbides, indicating that the reduced number of carbides (due to carbide coarsening on the account of dissolution of smaller particles) has affected the friction properties of the tempered steels.

Acknowledgements

The work presented was funded by the Austrian COMET Program (Project XTribology, no. 849109) and carried out at the “Excellence Centre of Tribology” (AC2T research GmbH) in cooperation with V-Research GmbH and Institute of Metals and Technology IMT.

References

- [1] Mutama K R 2013 *Proc. ASME Power Conf. (July 29th–August 1st 2013, Boston, MA)* vol. 1 (New York: ASME) paper no. POWER2013-98289 pp V001T04A009
- [2] Prat O, García J, Rojas D, Sanhueza J P and Camurri C 2014 *Mater. Chem. Phys.* **143** 754–64
- [3] Miao K, He Y, Zhu N, Wang J, Lu X and Li L 2015 *J. Alloys Compd.* **622** 513–23
- [4] Xu Y, Zhang X, Tian Y, Chen C, Nan Y, He H and Wang M 2016 *Mater. Charact.* **111** 122–7
- [5] Han Y, Xue X, Zhang T, Hu R and Li J 2016 *Mater. Sci. Eng. A* **667** 391–401
- [6] Liu F, Rashidi M, Johansson L, Hald J and Andrén H O 2016 *Scr. Mater.* **113** 93–6
- [7] Lu Q, Xu W and van der Zwaag S 2014 *Acta Mater.* **77** 310–23
- [8] Zhang H Y, Lu Y H, Ma M and Li J 2014 *Wear* **315** 58–67
- [9] Velkavrh I, Kafexhiu F, Klien S, Diem A and Podgornik B 2017 *Metall. Mater. Trans. A* **48** 109–25
- [10] Schindelin J, Arganda-Carreras I, Frise E, Kaynig V, Longair M, Pietzsch T, Preibisch S, Rueden C, Saalfeld S, Schmid B, Tinevez J Y, White D J, Hartenstein V, Eliceiri K, Tomancak P and Cardona A 2012 *Nat. Methods* **9** 676–82
- [11] Velkavrh I, Ausserer F, Klien S, Voyer J, Ristow A, Brenner J, Forêt P and Diem A 2016 *Tribol. Int.* **98** 155–71
- [12] Cabrera N and Mott N F 1949 *Rep. Prog. Phys.* **12** 163–84
- [13] Vodopivec F, Jenko M and Vojvodič-Tuma J 2006 *Metallurgija* **45** 147–53
- [14] Skobir D A, Vodopivec F, Jenko M, Spaić S and Markoli B 2004 *Int. J. Mater. Res.* **95**, 1020–4